International Journal of Pharmaceutics 643 (2023) 123214

Contents lists available at ScienceDirect

International Journal of Pharmaceutics

journal homepage: www.elsevier.com/locate/ijpharm

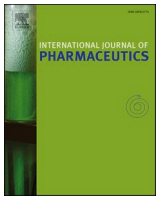

3D printed mucoadhesive orodispersible films manufactured by direct powder extrusion for personalized clobetasol propionate based paediatric therapies

Giuseppe Francesco Racaniello [a], Monica Pistone [a], Chiara Meazzini [b], Angela Lopedota [a], Ilaria Arduino [a], Rosanna Rizzi [c], Antonio Lopalco [a], Umberto M. Musazzi [b], Francesco Cilurzo [b], Nunzio Denora [a,*]

[a] Department of Pharmacy – Pharmaceutical Sciences, University of Bari Aldo Moro, Orabona St. 4, Bari 70125, Italy
[b] Department of Pharmaceutical Science, University of Milan, Via G. Colombo, 71, Milan 20133, Italy
[c] Institute of Crystallography-CNR, Amendola St. 122/o, Bari 70126, Italy

ARTICLE INFO

Keywords:
Oral Lichen Planus
Direct powder extrusion
3D printing
Mucoadhesive films
Clobetasol propionate
Paediatric therapy

ABSTRACT

The aim of this work is the development and production by Direct Powder Extrusion (DPE) 3D printing technique of novel oral mucoadhesive films delivering Clobetasol propionate (CBS), useful in paediatric treatment of Oral Lichen Planus (OLP), a rare chronic disease. The DPE 3D printing of these dosage forms can allow the reduction of frequency regimen, the therapy personalization, and reduction of oral cavity administration discomfort. To obtain suitable mucoadhesive films, different polymeric materials, namely hydroxypropylmethylcellulose or polyethylene oxide blended with chitosan (CS), were tested and hydroxypropyl-β-cyclodextrin was added to increase the CBS solubility. The formulations were tested in terms of mechanical, physico-chemical, and in vitro biopharmaceutical properties. The film showed a tenacious structure, with drug chemical-physical characteristics enhancement due to its partial amorphization during the printing stage and owing to cyclodextrins multicomponent complex formation. The presence of CS enhanced the mucoadhesive properties leading to a significant increase of drug exposure time on the mucosa. Finally, the printed films permeation and retention studies through porcine mucosae showed a marked retention of the drug inside the epithelium, avoiding drug systemic absorption. Therefore, DPE-printed films could represent a suitable technique for the preparation of mucoadhesive film potentially usable for paediatric therapy including OLP.

1. Introduction

Oral Lichen Planus (OLP) is a chronic mucocutaneous disorder of the stratified squamous epithelium affecting the oral mucous membranes (Canto et al., 2010). The disease occurs as a T-cell-mediated autoimmune condition, in which self-cytotoxic CD8+ T cells trigger apoptosis of basal cells of the oral epithelium (Eversole, 1997). Although its incidence is often reported in middle-aged patients, an important occurrence in the paediatric population is also observed (Boorghani et al., 2010; Laeijendecker et al., 2005).

The use of corticosteroids is to date the most indicated therapy for reducing the symptoms and local effects of autoimmune diseases of the oral mucosae (Ferguson, 1977). Topical corticosteroids, in fact, efficiently reduce inflammation-related symptoms (Plemons et al., 1990) by reducing leukocyte exudation and the formation of inflammatory mediators and preserving the integrity of cell membrane (Byyny, 1976). Clobetasol propionate (CBS) is a corticosteroid with strong anti-inflammatory, antipyretic, and vasoconstrictive properties (Oussedik et al., 2017) that is commonly used for the OLP topical treatment (Carbone et al., 2009). Topical application of CBS is promoted in clinical practice because it provides high benefits while maintaining minimal the possibility of side effects occurrence (Carruthers et al., 1975). However, CBS is characterized by low aqueous solubility which significantly limits its therapeutic efficacy (Sarfaraz Alam et al., 2016).

The administration of CBS in the buccal cavity occurs by using off-label semisolid preparations even if few works reports the possibility to develop mucoadhesive dosage forms such as tablets (Cilurzo et al., 2010) or oral lyophilizates containing mucoadhesive interpolymeric

* Corresponding author.
E-mail address: nunzio.denora@uniba.it (N. Denora).

https://doi.org/10.1016/j.ijpharm.2023.123214
Received 21 May 2023; Received in revised form 5 July 2023; Accepted 6 July 2023
Available online 8 July 2023

complexes (Garipova et al., 2018). However, both these approaches cannot result suitable when this pathology affects the paediatric population since tablets and semisolid formulations are poorly tolerated and mucoadhesive nanoparticles can be swallowed if the patient did not maintain the saliva in the buccal cavity for a sufficient period of time which assures the adhesion of the formulation on the mucosa (Morath et al., 2022). Moreover, an off-label use of semisolid preparations in paediatric patient's buccal cavity could adversely affect drug bioavailability and therapy outcomes (Cuzzolin et al., 2003). Hence, an unmet medical need in the paediatric population is evident, which could be addressed with the development of personalized oral formulations characterised by accurate and flexible dosages, sizes, and shapes suitable for children (Lafeber et al., 2022).

The aim of this study was to provide mucoadhesive oral films containing approximately 125 μg/dose of CBS, a dose deemed therapeutically appropriate and functional to ensure the OLP treatment (Cilurzo et al., 2010), in order to enhance paediatric patients' compliance toward therapy (Scarpa et al., 2017). In order to produce mucoadhesive oral films that accurately meet the personal needs of the individual paediatric patient, the 3D printing technique was used (Zema et al., 2017). In fact, among all techniques available to date for obtaining oral films, 3D printing ensures a better uniformity of active compounds and reduced operational units, allowing the continuous production process (Palezi et al., 2022). Therefore, the 3D printing technique can be used to produce polymer matrices with greater precision for the incorporation of the active compound (Preis et al., 2015). The concentration of active ingredients can be fully customized by changing the print settings and geometry, producing a final pharmaceutical form on demand according to individual patient needs (Boniatti et al., 2021; Khalid et al., 2021).

To date, several natural and synthetic hydrophilic polymers, such as hydroxypropylmethylcellulose (HPMC) (Polamaplly et al., 2019), maltodextrin (Musazzi et al., 2018b), polyvinyl alcohol (PVA)(Wei et al., 2020), polyethylene oxide (PEO) (Chung et al., 2022), polylactic acid (PLA)(Liu et al., 2020), and polyvinylpyrrolidone (PVP) (Dores et al., 2020) have been investigated for the manufacture of 3D printing-based pharmaceutical forms for personalized therapy (Azad et al., 2020). Among them, PEO and HPMC have been already studied for the design of mucoadhesive oral films (d'Angelo et al., 2017; Mašková et al., 2020; Russo et al., 2016).

Indeed, efficient oromucosal administration requires a prolonged contact time of the drug on the epidermal or mucosal surface, preventing saliva elution and thus allowing the continuous treatment of local conditions (Jiang et al., 2017). Therefore, the dosage form must possess mucoadhesive properties that increase the exposure time of the drug to the mucosae, improving its therapeutic efficacy and minimizing its toxicity (Nair et al., 2022). Even if HPMC and PEO exhibit quite good mucoadhesive properties they are often used in combination with other polymeric materials that can enhance their interactions with mucins (Bernkop-Schnürch, 2005; Russo et al., 2016; Salamat-Miller et al., 2005).

Chitosan (CS) is a linear polysaccharide copolymer with mucoadhesive properties provided by –OH and $–NH_2$ groups, leading to the formation of hydrogen and covalent bonds with the cysteine groups of the mucosal layers (Cheung et al., 2015). This polymer is widely used in the pharmaceutical field not only because of its strong mucoadhesive properties, but also because its biocompatibility and toxicity characteristics make it safe to use (Tejada et al., 2017).

In addition, to improve the aqueous solubility of CBS, hydroxypropyl-β-cyclodextrin (HP-β-CD) was included in the obtained formulation. HP-β-CD has been widely used in pharmaceutical formulations with the purpose of increasing the aqueous solubility of poorly soluble drugs by stabilizing them through the formation of inclusion complexes (Racaniello et al., 2021). CDs are a class of cyclic oligosaccharides consisting of six, seven or eight glucose units linked by α-(1,4)-glycosidic bonds. The spatial arrangement of the molecules gives CDs a hydrophilic shell and a hydrophobic core. It takes the shape of a truncated cone, which can be used as a host molecule to encapsulate insoluble compounds of appropriate size (Loftsson et al., 2005). In addition, the formation of cyclodextrins multicomponent complexes (drug, CD, and polymer) in which the polymer can improve the stability of the drug-CD complex has been demonstrated in the past by the formation of ternary complexes that can greatly increase the aqueous solubility of the drug (Pistone et al., 2022). In this case, HP-β-CD is also responsible for masking the taste of the drug in the final formulation by hindering its interaction with taste receptors (Rincón-López et al., 2021).

In order to make the resulting pharmaceutical forms fully customizable, the mucoadhesive films were produced through an innovative 3D printing technique, Direct Powder Extrusion (DPE) (Fanous et al., 2020; Ong et al., 2020). The DPE technique can obtain the final pharmaceutical form starting directly from medicated powder pellets or blends, bypassing the intermediate step of thermoplastic filament formation provided by other printing techniques currently in use and thus preserving the active from the possibility of degradation (Goyanes et al., 2019; Pistone et al., 2022). An additional advantage of this technique is the possibility of using different dosages of drug, even with higher concentrations of active ingredient, allowing complete customization of the final pharmaceutical form, making it adherent to the individual patient's needs (Pistone et al., 2023).

Therefore, in this work, CBS-loaded mucoadhesive films were produced by the DPE 3D printing technique starting from different powder mixtures. Subsequently, the obtained films were fully characterised regarding chemical and physical characteristics in order to evaluate their differences and identify the best formulations. In addition, an evaluation of mucoadhesive and tensile properties and in vitro permeation and retention characteristics was performed in order to validate the obtained mucoadhesive films as possible drug delivery systems in paediatric OLP therapy.

2. Materials and methods

2.1. Materials

CBS and HP-β-CD (Cavasol W7, HP-β-CD with MW = 1540, molar substitution degree SD = 7) were purchased from Farmalabor Srl (Canosa di Puglia, ITALY). AFFINISOL™ HPMC HME 15 LV (hydroxypropyl methylcellulose) was gifted by Pharma Solutions – Nutrition & Biosciences Italy (Milan, ITALY). PEO (Polyox WSR N10, MW = 100.000) was purchased from DuPont, Italy (Milano, ITALY). Chitosan (low molecular weight) and Crude (Type II) mucin from porcine stomach were purchased from Sigma-Aldrich (Merck, Darmstadt, GERMANY). Potassium Phosphate Dibasic was purchased from Honeywell Fluka Italia (Rodano, ITALY). For the analysis, distilled and purified water (resistivity of 18.2 MΩ.cm at 23 °C) was obtained by the purification system Milli-Q (Purelab DI, MK2) (Elga, High Wycombe, UK). Acetonitrile and methanol were purchased by VWR S.r.l. (Milano, ITALY). All solvents were of analytical grade, unless specified.

2.2. Quantitative analysis of CBS by HPLC method

The concentration of CBS was determined by HPLC (HP 1100, ChemStations, Agilent Technologies, USA), modifying the analytical method proposed by Kamberi et al. (Kamberi et al., 2008). Compound separation was carried out using a reverse-phase column (Inertclone 5 μm, ODS, 100 A, 150 × 4.6, Phenomenex Inc., USA) and HPLC-grade water/acetonitrile as mobile phase. The gradient applied during the analysis was: 0 min, B: 52%; 2.5 min, B: 65%; 2.6 min, 68%; 4.9 min, B: 68%; 10 min, B: 52%. The flow rate was 1.0 mL/min, and the injection volume was 20 μL. The retention time of CBS was around 6.3 min. The drug concentration was determined at 240 nm from calibration curves in the range of 0.05–1 μg/mL (R^2 = 1.000).

2.3. Phase solubility studies

The phase solubility study of CBS with HP-β-CD was performed according to the Higuchi-Connors method (Cutrignelli et al., 2014a). Briefly, 2 mL samples were prepared with solutions of different concentrations of HP-β- CD covering a concentration range from 0.0064 to 0.19 M. The concentration of the drug was determined by HPLC method. An excess amount of the drug was added to each solution and the resulting suspensions were sonicated at 37 °C for 2 min. They were then allowed to settle for 48 h in a thermostatic bath at 37 °C with constant oscillation. After reaching equilibrium, the samples were centrifuged at 10,000 rpm for 15 min, and the supernatant was filtered through 0.45-μm cellulose acetate membrane filters (CA) and analysed. The concentration of CBS was determined by HPLC according to the method described above. A solubility diagram was obtained by plotting the molar concentration of the drug against the HP-β-CD molar concentration. The complexation constant ($Kc_{1:1}$) was calculated using the Higuchi-Connors method (Eq. (1)):

$$Kc_{1:1} = \frac{P}{S_0(1-P)} \quad (1)$$

where:

S_0 = Intrinsic solubility of CBS in water.
P = Slope of the phase solubility diagram.

Moreover, a solubility study was carried out in the presence of 3% (w/w) HP-β-CD, 15% (w/w) CS, 81.45% (w/w) PEO, and 0.35 % (w/w) HPMC to see if the formation of a multiple polymer system could further increase the solubility of the drug. The same procedure was carried out as previously described.

2.4. Inclusion complex stoichiometry determination (Job's plot method)

The HP-β-CD/CBS inclusion complex in aqueous solution was analyzed using the continuous variation method to verify stoichiometry (Cutrignelli et al., 2014b). The difference between the absorbance intensity with and without CD (ΔA) at 260 nm was determined using mixtures of CBS: CD with different molar ratios (from 0 to 1) while keeping the total molar concentration of the species constant. The mixtures were prepared using equimolar (1.0×10^{-4} M) Acetonitrile/H_2O (50/50 v/v) solutions of CBS and HP-β-CD. The ΔA × [CBS] was plotted against r, where r was defined by the following equation:

$$r = \frac{[CBS]}{[CBS] + [CD]} \quad (2)$$

2.5. Preparation of powder blends

Four samples consisting of polymer powder blends of different concentrations of CS and PEO with a constant drug concentration (CBS 0.20 % w/w) were prepared. In each mixture, HP-β-CD and HPMC to improve drug solubility were employed. The final compositions of the mixtures are reported in Table 1.

Each component was sieved three times through a 355 μm mesh sieve to ensure better dimensional uniformity and mixing of the powder. The powders were then mechanically stirred at 67 rpm for approximately one hour using a Turbula Willy A. Bachofen GmbH (Nidderau, Germany). The resulting powder mixtures were dried overnight in an oven at 40 °C.

Table 1
Composition of the powder mixtures.

Samples	CBS	PEO	HPMC (% w/w)	CS	HP-β-CD
Blend 1	0.20	86.45	0.35	10.00	3.00
Blend 2	0.20	81.45	0.35	15.00	3.00
Blend 3	0.20	71.45	0.35	25.00	3.00
Blend 4	0.20	66.45	0.35	30.00	3.00

2.6. Direct powder extrusion 3D-printing

The films were printed using a 3DForMe® 3D printer specifically designed for pharmaceutical manufacturing. The model of the film was created using Fusion360 software from CAD, which allowed the creation of stereolithography (.stl) files that were then exported to the 3D printer software (Ultimaker Cura). The stereolithography file describes the geometry of the object, while all other parameters are set directly in the Ultimaker Cura software. A cylindrical geometry was chosen to obtain a circular 3D printed film with dimensions of 20 mm (diameter) × 0.3 mm (height). A parallelepiped geometry was used for characterization to obtain rectangular 3D printed films with a dimension of 50 mm (length) × 20 mm (width) × 0.3/0.6 mm (height). This size made it possible to obtain film with the required weight of 62.5 mg. The parameters set in the software for printing were: infill 40% with infill pattern Concentric, high resolution with brim, without raft, travel speed 5 mm/s, print speed 5 mm/s, number of shells 2, layer height 0.125 mm, floor temperature 40 °C and extrusion temperature of 170 °C. The prepared powder mixture was placed in the extruder hopper of the 3D printer, which was specially designed with a direct single-screw powder extruder and a nozzle diameter of 0.8 mm. The extruder design was based on a single-screw HME, and the rotation speed was controlled by the 3D printer's software. In addition, the extruder nozzle moves in three dimensions to create objects with a layered texture. During printing, all the blends met the same extrusion temperature conditions set in the software. At the end of each print, the extruder was disassembled, removed from the screw, and cleaned to avoid contamination between the blends.

2.7. Extruded filaments characterization

Prior to the printing phase, preliminary studies were conducted to evaluate the behaviour of the four blends during extrusion and the properties of the extruded filament. In the present study, a 3DForMe® 3D printer (Farmalabor, Canosa, ITALY) was used, consisting of a feed hopper, a single-screw extruder and temperature measurement and control systems. 2 g of each blend were placed in the hopper, and the filament formed by extrusion was operated at 170 °C. At the end of each extrusion process, the filaments were weighed to calculate the yield of the process and visually inspected to assess their suitability for use in obtaining the final pharmaceutical form. From each blend, five pieces of 2 cm length were cut, weighed, and studied to demonstrate the homogeneity of the filament printed. Visual inspection and the amount of CBS were considered. The pieces were dissolved in 4 mL of acetonitrile and stirred overnight. After appropriate dilution, the solutions were analyzed by HPLC to calculate the amount of CBS in each piece.

2.8. Solid state characterization of powder blends

Obtained printed films were characterized in the solid state, together with the pure drug and the physical blend consisting only of the excipients. They were analyzed by Fourier transform infrared spectroscopy (FT-IR), differential scanning calorimetry (DSC) and powder X-ray diffraction (PXRD). For the FT-IR analysis, KBr pellets (2% of the sample) were analyzed using a FT-IR 1600 Perkin Elmer spectrophotometer. Data were acquired between 4000 cm^{-1} and 400 cm^{-1}. Differential scanning calorimetry (DSC) of the different samples was performed using a Mettler Toledo DSC822 instrument. About 5–10 mg of the sample was heated in an aluminium pan at a heating rate of 5 °C/min from 0 °C to 250 °C under N_2 flow. The analysis was conducted by presenting a first phase of heating from 0 °C to 250 °C, a second phase of cooling from 250 °C to 0 °C, and a third phase of heating from 0 °C to

250 °C, in order to check the possible degradation of the polymers and the drug during the printing steps. An empty pan was used as the reference. The X-ray powder diffraction patterns were collected using a Rigaku Rint2500 rotating Cu anode working at 50 kV and 200 mA in Debye–Scherrer geometry. The diffractometer was equipped with an asymmetric Johansson Ge (1 1 1) crystal to select monochromatic CuKα_1 radiation (λ = 1.54056 Å) and a Rigaku D/teX Ultra silicon strip detector. The range from 5 to 70° (2ϑ) was collected with a 0.02° (2ϑ) step size and counting time of 6 s/step. Each powder sample was introduced into a glass capillary (diameter, 0.5 mm) and mounted on the axis of the goniometer. The capillary was rotated during the measurement to improve the randomization of the orientations of the individual crystallites and reduce the effect of the preferred orientation.

2.9. Characterization of mucoadhesive films

The physical dimensions of the printed films were assessed using a digital slide gauge (Hitech Diamond). The morphology of the film obtained during the printing stage was evaluated using an electrical scanning microscope (SEM) operating at 20 kV (Hitachi TM 3000 Tabletop SEM). Furthermore, a Chemical Microanalysis test was conducted on the samples to confirm the presence of F and Cl, which are elements present only in the CBS structure, and thus investigate the dispersion of the drug within them. The surface of each printed film was analyzed using a Swift ED3000 Oxford Instrument with AZtecOne software. Finally, 10 mucoadhesive oral films were dissolved in acetonitrile to evaluate the actual CBS loading, in order to verify the presence of a therapeutic amount of CBS inside (125 μg). Each film was placed in 10 mL acetonitrile and stirred overnight at room temperature. Finally, after appropriate dilution, the drug concentration was assessed using HPLC, as previously reported.

2.10. Solid state characterization of mucoadhesive films

The printed films were characterized by FT-IR, DSC, and PXRD following the same procedures previously described for the solid-state characterization of the blend. Before analysis, the printed formulations were fragmented, ground, and sieved.

2.11. Mucoadhesive properties

Characterization of film mucoadhesive properties were performed by using an Instron 5965 texture analyzer (Instron, UK), equipped with a 50 N load cell. The samples of each (reported in Table 2) were attached to the mobile steel punch by cyanoacrylate glue. Mucin compacts, weighting 130 mg, were attached with cyanoacrylate glue to a steel plate fixed at the bottom of the tensile apparatus and hydrated with 80 μL water for 5 min, in order to obtain a jelly superficial mucin stratum. The compacts were preliminarily obtained applying a compression force 11 tons for 60 s, by using a hydraulic press (Glenrothes, UK) equipped with flat faced punches and having a die diameter of 11.28 mm. At the experiment start, upon making contact between the sample and the hydrated mucin, a constant force of 1.3 N was imposed for 120 s. The mucoadhesive performance of the tested materials was determined by measuring the detachment force (DF) required to separate the sample from the mucin compact (maximum detachment force; DF_{max}) upon an elongation of 10.0 mm at the constant rate of 0.1 mm/s. The area under the curve (AUC) of the detachment force versus the elongation was also determined to represent the work or energy required for the detachment of the sample from the mucin.

Table 2
Composition and dimensions of the forms used for the test.

Form.	Blend	Dimension length × width × height (mm)
1	2	50 × 20 × 0.3
2	2	50 × 20 × 0.6
3	3	50 × 20 × 0.6

2.12. Tensile properties

Tests were conducted according to ASTM International Test Method for Thin Plastic Sheeting (D 882-02) using an Instron 5965 texture analyzer (Instron, UK), equipped with a 50 N load cell. The samples were 50 × 20 mm strips.

Each test strip was longitudinal by placed in the tensile grips on the texture analyzer. Initial grip separation and the crosshead speed were 20 mm and 12.5 mm/min, respectively. The test was considered concluded at the film break. Tensile strength (TS) was calculated by dividing the maximum load by the original cross-sectional area of the specimen. Percent elongation at break (E%) was calculated according to the following Eq. (3):

$$E\% = \frac{L - L_0}{L_0} \times 100 \quad (3)$$

where L_0 is the initial gage length of the specimen and L is the length at the rupture.

Elastic modulus or Young's modulus (Y) was calculated as the slope of the linear portion of the stress–strain curve. Tensile energy to break (TBE) was defined by the area under the stress–strain curve. The results were expressed in MPa.

2.13. In vitro permeation study

The Franz diffusion cells are used to investigate the kinetics of drugs release rate in vitro. This cell comprises two compartments, one containing the active component (donor vehicle) and the other containing a receptor solution, separated by a slice of porcine esophageal epidermis. The vertical cells used in the actual set of experiments had a wider column than the original Franz-type diffusion cell, and the bowl shape was removed. They had a diffusion area of 0.636 cm^2 and a 3.0 mL (approx.) receptor compartment. The receptor volume of each cell was equipped with a magnetic stirrer and individually calibrated.

The permeation studies were performed using the fresh porcine esophageal tissue obtained by a local slaughterhouse. The mucosae epithelium was separated by mucosal specimens using a scalpel and stored at 2–8 °C until use for not more than 24 h (Casiraghi et al., 2020). Prior to experiments, the mucosae epithelia were thawed at room temperature, and cut into squares of about 4.5 cm^2. The integrity of esophageal epithelia was visually checked before the experiments.

A 2.0 cm^2 circular sample, obtained from film by a precision die cutter, was gently applied to the esophageal epithelium specimen, preliminary hydrated with 80 μL of HPLC-grade water to facilitate the contact with the mucosae. Then, the assembly was mounted on the receiver compartment of the Franz diffusion cell whose receptor compartment was filled with sterile 0.9% sodium chloride aqueous solution (Eurospital S.p.A., Italy). Special care was given to avoid air bubbles between the solution and the epidermis in the receptor compartment. The upper and lower parts of the Franz cell were sealed with Parafilm® (Pechiney Plastic Packaging Company, USA) and fastened together by means of a clamp, with the epidermis acting as a seal between the donor and receptor compartments. The system was kept at 37 °C with a circulating water bath throughout the experiment. At predetermined times (1, 3, 5, 7 h), 200 μL samples were withdrawn from the receiver compartment and replaced with fresh receiver medium. Samples were analyzed by HPLC according to the above-described method. The values were the average of parallel experiments performed in triplicate. The cumulative amount permeated through the esophageal mucosae per unit area (Qt, perm) was calculated from the drug

concentration in the receiving medium and plotted as a function of time.

2.14. In vitro retention study

At the end of the permeation experiments, the concentration of opioid retained into the epidermis (Q7h, ret) was quantified by the following procedure. The esophageal epithelium was removed from the Franz diffusion cell and stripped (Transpore®, 3 M, USA) to eliminate the unabsorbed formulation. Then, each side of the membrane was gently treated with 5 mL of MeOH to wash out the unabsorbed drug. Subsequently, the sample was thinly sliced and placed in 5 mL of fresh MeOH. The suspension was soaked in a probe-sonicator (UP200St, Hielscher, Germany) for 10 min and then maintained for 24 h at 2–8 °C. Finally, the supernatant was centrifuged at 7000 rpm, 25 °C for 5 min (Z326K, Hermle LaborTechnik GmbH, Germany) to eliminate suspended materials and then, analyzed by HPLC. Q7h, ret was expressed as micrograms of CBS per milligrams of esophageal epithelium.

2.15. Ex-vivo mucoadhesion and dissolution test

The wash-off method was used to measure the mucoadhesive and dissolution properties of the Form. 2 and 3. In detail, an appropriate sample with dimensions of 2 cm (diameter) × 0,3 mm was 3D printed starting from Blend 2 and Blend 3 to standardize the membrane surface area of contact and validate the assay. The obtained samples were placed on a 2 × 3 cm section of the animal mucosae and fixed on a 45° inclined surface. Animal mucosae, derived from porcine esophagus, was freshly obtained from a local slaughterhouse (Bari, Italy). The mucosae epithelium was separated by mucosal specimens using a scalpel, cleaned, and stored at 4 °C in phosphate buffer solution (pH 7.2) before use (Casiraghi et al., 2020). Then, 60 mL of the simulated salivary fluid solution was poured using a syringe connected to a pump onto the sample placed on the mucosae at a constant flow rate of 1 mL/min to simulate salivary flushing. At time intervals of 5 min for a total time of 60 min, 300 μL were withdrawn from the washing solution and replaced with the same volume of simulated salivary fluid solution. The obtained samples, after appropriate dilutions, were analyzed by the previously reported HPLC method in order to assess the concentration of CBS removed from the esophageal mucosa over time. Determination was performed by an indirect method using the following Eq. (4):

$$Mucoadhesion\,(\%) = \frac{CBS\,(Total\ \ Amount) - CBS\,(collected\ \ sample)}{CBS\,(Total\ \ Amount)} \times 100 \quad (4)$$

2.16. Stability studies

The samples were stored in a Climacell 222 – ECO line climatic chamber (MMM Group, Semmelweis Strasse, München, Germany) at 25 °C and 60% relative humidity (RH) for 3 months. The printed films were packaged in amber glass bottles and closed using plastic screw caps. They were monitored using DSC analysis and CBS content over the storage period.

2.17. Statistical analysis

Experimental data are reported as mean ± standard deviation (SD). Statistical analysis was conducted using JMP® Pro 16 (Marlow, UK). Statistically significant differences in obtained results were determined by Tukey-Kramer post-hoc tests after One-way ANOVA analysis.

3. Results and discussions

This work employed the new 3DForMe® printer based on the DPE printing technique to obtain mucoadhesive films capable of oral delivery of CBS in OPL therapy. In order to achieve a rapid dissolution of the finished pharmaceutical form in the oral cavity different hydrophilic polymers of certain effectiveness were used in the initial powder matrix. Moreover, a notoriously mucoadhesive polymer such as CS was added to the films initial powder mixture. Therefore, different powder mixtures composed of CBS, HPMC, HP-β-CD, PEO and CS at different concentrations were first characterized and then extruded through the DPE technique. A complete solid-state characterization of the different blends and the printed films was described, along with an evaluation of the mucoadhesive and tensile properties of the printed films and the in vitro permeation and retention characteristics.

3.1. CBS phase solubility studies

Phase solubility studies of the drug were performed in the presence of HP-β-CD, which allowed evaluation of the stability constant and prediction of the stoichiometric ratio of the CBS/HP-β-CD complex. Pure CBS has an intrinsic solubility of 2 μg/ml in water. The phase solubility diagram showed a significant and linear increase in CBS solubility with increasing HP-β-CD concentration (Fig. 1). The drug showed a solubility of 566.46 μg/mL in the presence of HP-β-CD at a concentration of 0.194 M. The regression analysis ($R^2 = 0.9974$) describes an AL-type curve, according to the Higuchi-Connors classification, with a slope of less than 1, which could be associated with a 1:1 M ratio between CBS and HP-β-CD. Using the Higuchi-Connors Connor's equation, a stability constant of 1335.74 M^{-1} was calculated, indicating a good interaction between CBS and HP- β -CD. Indeed, stability constants between 50 and 2000 M^{-1} are considered advantageous. (Loftsson et al., 2005).

The addition of HPMC and PEO at HP-β-CD solution significantly improved the aqueous solubility of CBS, confirming that the use of hydrophilic polymers increased the CD complexation efficiency for drugs (Medarević et al., 2015). In all samples containing the cyclodextrins multicomponent complex (hydrophilic polymers/HP-β-CD/drug), a significant increase in aqueous solubility of CBS was observed in comparison to solution containing the HP-β-CD. Samples in which HPMC was also present showed higher drug solubility enhancement, which was found a 25-fold increase compared with samples presenting the binary inclusion complex (Fig. 2). Based on these results, it could be stated that hydrophilic polymers and HP-β-CD showed a synergistic effect in enhancing CBS solubility.

3.2. Job's plot method

Job's plot method was applied to determine the stoichiometry of the inclusion complexes. The maximum deviation value of ΔA indicated the stoichiometry of the CBS/HP-β-CD inclusion complex. The change in absorbance (ΔA) × [CBS] was calculated using equimolar (1.0×10^{-4} M) Acetonitrile/H_2O solutions of CBS and CD solutions. As shown in Fig. 3, the maximum value at r = 0.5, with a symmetrical shape, demonstrated the presence of a 1:1 complex stoichiometry.

3.3. Extruded filaments characterization

A visual evaluation was carried out on the filaments obtained from extrusion by HME of four different powder blends. The blends differed in the percentage (w/w) of PEO and CS present in their formulation. Analyzing the filament obtained from Blend 1, it was observed that a high percentage of PEO in the composition resulted in a filament with a structure that was too brittle to be used in 3D printing, which also presented difficulties in solidification by quenching (Fig. 4A), which leads to the formation of a film with areas of under-extrusion (Fig. 4B). As shown in Fig. 4A, the filament obtained from the extrusion of Blend 2 and Blend 3 were defect-free, making them preferred for deployment in the next stage of 3D printing of films (Fig. 4B), proving to be flexible but firm in consistency. DPE requires that the powders have a certain degree of fluidity and homogeneity to ensure that the flow through the extruder is uniform (Spath and Seitz, 2014). The filaments obtained from Blend 4,

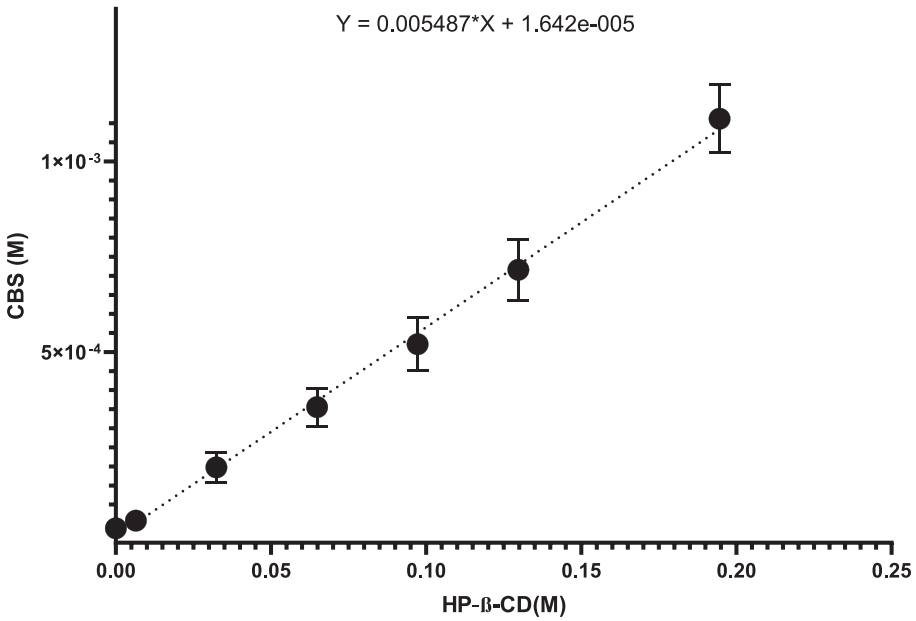

Fig. 1. Phase solubility studies of CBS/HP-β-CD complex.

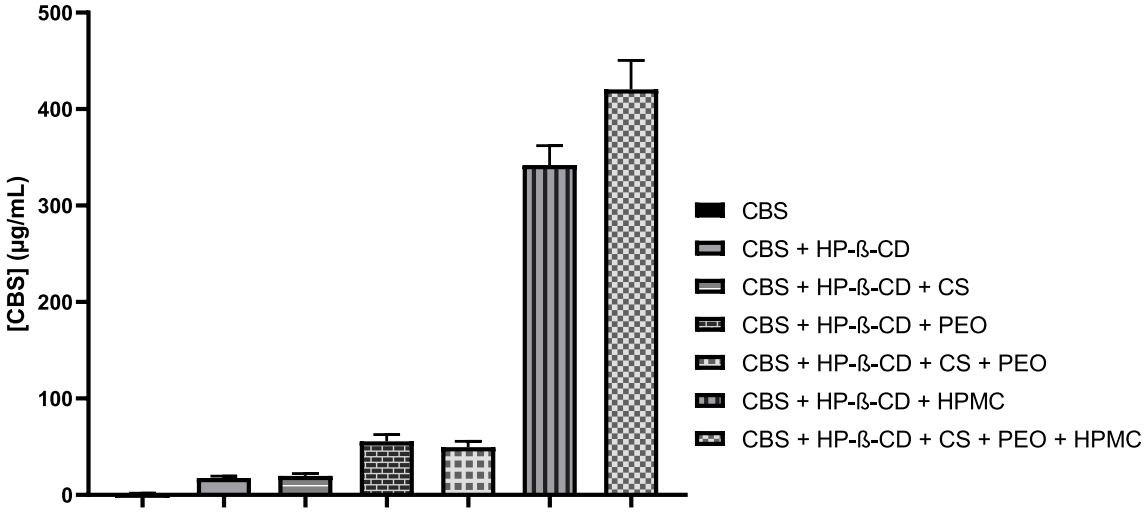

Fig. 2. Aqueous solubility of CBS in the presence of binary (CD/Drug) and cyclodextrins multicomponent complexes (hydrophilic polymers/CD/drug). The analysis was conducted in triplicates.

on the other hand, had a high percentage of CS, which proved to be structurally too rigid and not malleable (Fig. 4A), and thus unsuitable for the purpose of 3D printing, leading to the formation of films with irregular surfaces and varying thicknesses owing to the difficulty of handling the extrudate (Fig. 4B).

Thereafter, further tests to assess the weight and homogeneity of the CBS content were carried out for all blends. For all filament fragments (2 cm), the percentage of drug was in the range of 0.182–0.195 % w/w. However, the average of the values obtained was very close to the value of the theoretical concentration, thus demonstrating that the adopted process was not detrimental to the drug (Table 3) despite contact with the high temperatures of the extruder. The weight variations that characterize the filaments obtained from Blend 1 and Blend 4 could be the result of under-extrusion and over-extrusion, respectively.

Evaluating the results obtained from characterization tests carried out on the extruded filaments, Blend 2 and Blend 3 were found to be the most suitable for printing by the DPE technique, owing to the ease of processing the extrudate and homogeneity in weight and CBS content. Therefore, all subsequent studies were conducted exclusively on films obtained from Blend 2 and Blend 3.

3.4. Direct powder extrusion 3D-printing

A single-screw extruder-printer model was used for the DPE. The mixed powder was filled into the hopper, heated to a certain temperature, and used for direct printing of tablets. This innovative printing technique overcomes the limitations associated with conventional tablet printing systems (Pandey et al., 2020) and with established printing processes such as HME. By eliminating the preparatory HME step and subsequent FDM printing, the DPE printing process becomes simpler and faster. In fact, the overall process of printing a film takes about 3 min. In addition, by eliminating the intermediate steps, the amount of raw material waste has been greatly reduced. The design of the extruder, with a vertical orientation and an appropriate distance from the hopper, facilitates the flow of powder into the screw. A functional amount of powder can be filled into the hopper to ensure the production of 1–15

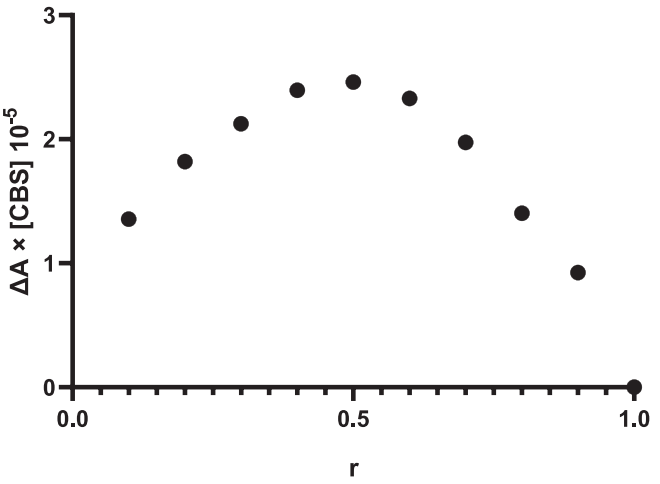

Fig. 3. Job's plot diagram for stoichiometry determination of CBS/HP-β-CD inclusion complexes.

films for single cycle keeping the set dimensional values unchanged. This makes this 3D printing process suitable for formulating personalized mucoadhesive film in OLP therapy.

Blend 2 and Blend 3 were found to be suitable for DPE 3DP. The presence of cyclodextrin tends to moisten the powder with increasing residence time in the printer, creating vacuum zones along the screw and blocking the extruder. The presence of a plasticizer and glidant agent as PEO assisted the printing process and promoted the flow of the powder within the screw. The resulting CBS based printed films had cylindrical or rectangular shapes and good adhesion between the printed layers (Fig. 5). The obtained printed films showed two distinct faces, one rougher, given by the deposition and shaping of the extrudate during the printing stage, and one flatter, corresponding to the face lying on the work bed.

3.5. Characterization of mucoadhesive films

The obtained mucoadhesive films exhibited good uniformity in physical dimensions, with the diameter and height values deviating slightly from the respective values set on the digital model (20 mm × 0.3 mm). The mean diameter ranged from 19.88 mm to 20.50 mm, and the mean height ranged from 0.292 mm to 0.312 mm. The mean mass was described as values ranging from 62.32 to 62.67 mg. All mucoadhesive films had mechanical properties that were functional for packaging and handling. From the content uniformity test, the drug concentration present in 10 mucoadhesive films was obtained, confirming the closeness to the theoretical drug value (125 μg) and demonstrating no degradation of the drug during extrusion.

The SEM images show the surface and transverse planes of the two films (Fig. 6). In the cross-section, a three-dimensional layer-by-layer structure, which is characteristic of mucoadhesive films obtained by 3D printing, can be seen (Fig. 6C). Each layer has a thickness of 0.15 mm, as determined by the printing parameters. The surface plane shows the concentric geometry of the selected infill.

The data obtained from the chemical microanalysis show a homogeneous presence of the elements Cl (green in Fig. 6E) and F (red in Fig. 6F), which, being atoms exclusively present in the structure of the drug, indicating an equal distribution of CBS within the printed mucoadhesive films (Fig. 6D). These results showed that CBS was homogeneously present inside the obtained preparation, thus avoiding possible phenomena of therapeutic ineffectiveness or possible overdosage.

3.6. Solid state characterization of printed mucoadhesive films

The possible amorphization of the drug during extrusion was verified by solid-state characterization studies of the printed mucoadhesive films. Using FT-IR, the characteristic peaks in the CBS spectrum were observed at 1063 (ether), 1606 (C═O), 1662 (C═C) and 1735 (Ester C═O) cm^{-1} (Fig. 7). The presence of these peaks was confirmed in the medicated blend spectra of each formulation. The peaks around 3300 cm^{-1} are characteristic of HP-β-CD, as observed in the complex, physical mixture, and extruded blend (Fig. 7). Analyzing the spectrum in comparison with the printed mucoadhesive films prepared from the above blends, we can observe a relative broadening of the HP -β- CD peak in the range 3350–3100 cm^{-1}. This widening could be attributed to the interaction of HP -β- CD with HPMC and CBS during printing (Thiry et al., 2017). The same observation can be made for the CBS peaks

Table 3
Average CBS concentrations (%) present within different HME filaments.

Filament fragments	Weight* (g)	Theoretical CBS (% w/w)	Measured CBS* (% w/w)
Blend 1	0.014 ± 0.001	0.20	0.188 ± 0.005
Blend 2	0.016 ± 0.001	0.20	0.195 ± 0.002
Blend 3	0.017 ± 0.002	0.20	0.196 ± 0.008
Blend 4	0.021 ± 0.002	0.20	0.182 ± 0.011

*The value is the average of 5 fragments, ± is the standard deviation.

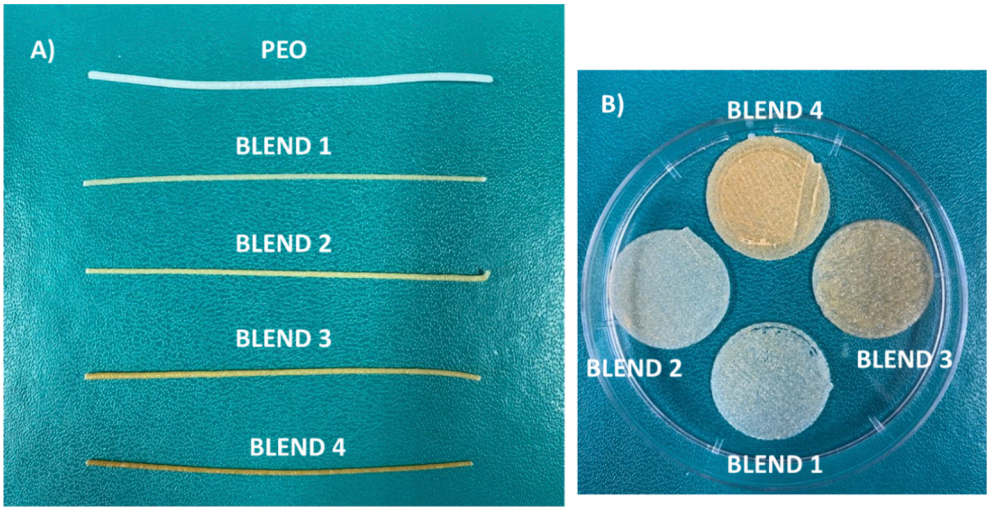

Fig. 4. Filaments obtained from the four different blends used (A) and respective printed films (B).

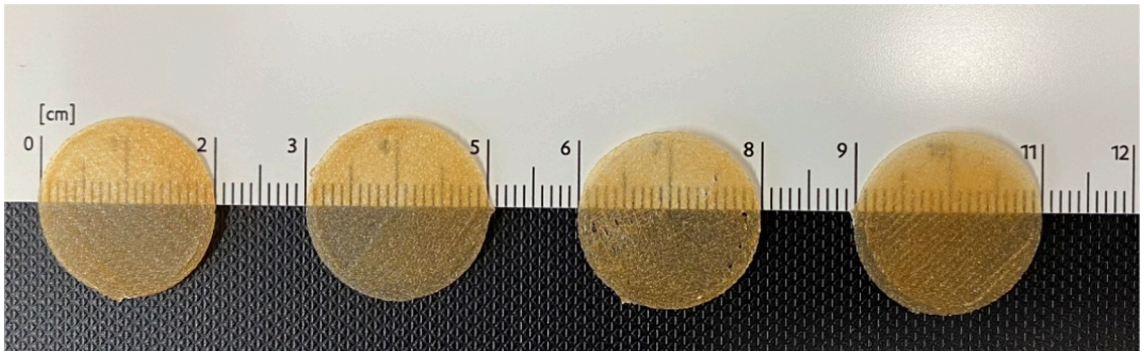

Fig. 5. Uniformity of dimensions of mucoadhesive film derived from the extrusion of Blend 3.

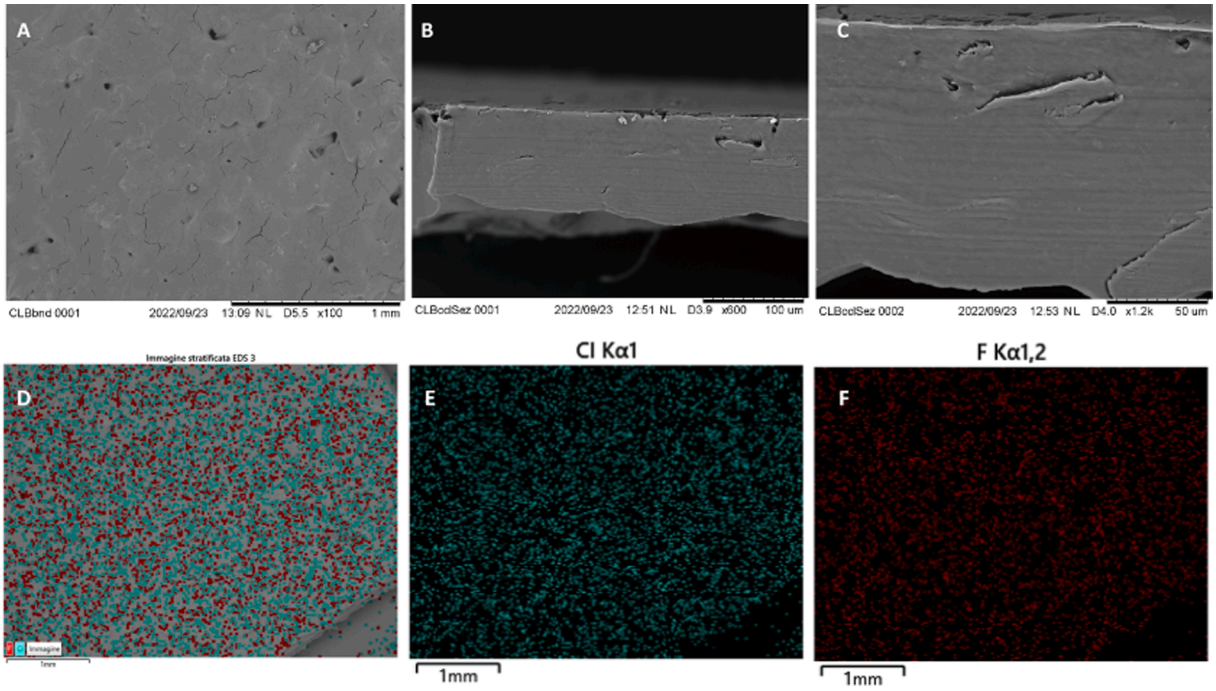

Fig. 6. SEM images of the printed film surface (A) and film cross-section (B – C). Surface chemical microanalysis of the printed mucoadhesive films (D) with images related to the presence of the element Cl (E) and F (F).

between 1600 cm^{-1} and 1800 cm^{-1} and between 1250 cm^{-1} and 1100 cm^{-1}. The absence of important peaks characteristic of the stretching of the ester and carbonyl groups of the drug could indicate a possible amorphization of the drug inside the printed film and/or an interaction between the drug and HP -β- CD (Lodagekar et al., 2019). These results confirm the formation of intimate complexes of HP-β-CD, CBS, and HPMC.

A second test to verify this condition was performed using DSC. CBS showed an endothermic peak at 220 °C, which is indicative of its crystalline nature (Fig. 8). In contrast, the peak at 220 °C was completely absent in the thermogram of the film, probably because of the amorphization of the drug during the printing phase and/or the formation of an inclusion complex between CBS and HP-β-CD.

In Fig. 9, the powder diffraction patterns of CBS, medicated blend, and corresponding printed mucoadhesive films are reported. The sharp peaks present in the diffraction pattern of the pure CBS powder indicated its crystallinity. Drug-related peaks were still observable in the diffractogram of the printed film, indicating the incomplete amorphization of the drug and the incomplete complexation with HP-β-CD.

3.7. Mucoadhesive properties

The test was performed to provide a complementary characterization of the films mucoadhesive properties. Indeed, while the falling technique using the porcine mucosae provided a prevision of the in vivo residence time, this test gave an idea of the initial bonding and provide a quantitative measure of the interaction between the film and a commercially available mucin. As shown in Table 4 and Fig. 10, significant differences in films mucoadhesive properties were observable. During the early part of the profile, the DF increased in all formulations as a function of the elongation until a maximum value was reached. A plateau was observable in all formulations due to the gradual detachment of the film, which resulted in a slightly changing of the contact area between the film and the mucin compact (Cilurzo et al., 2003). Finally, the DF rapidly dropped as a consequence of the complete detachment. As evident from Fig. 10, the intensity of plateau phase was influenced by the film composition. In particular, the higher the CS concentration, the longer the plateau phase. The detachment force of Form. 3, which has a higher CS concentration, was 1.2-time higher than Form. 1 and Form. 2 ($p < 0.01$). This evidence agreed with previously published results (Morales and McConville, 2011). Such a trend is also observable in terms

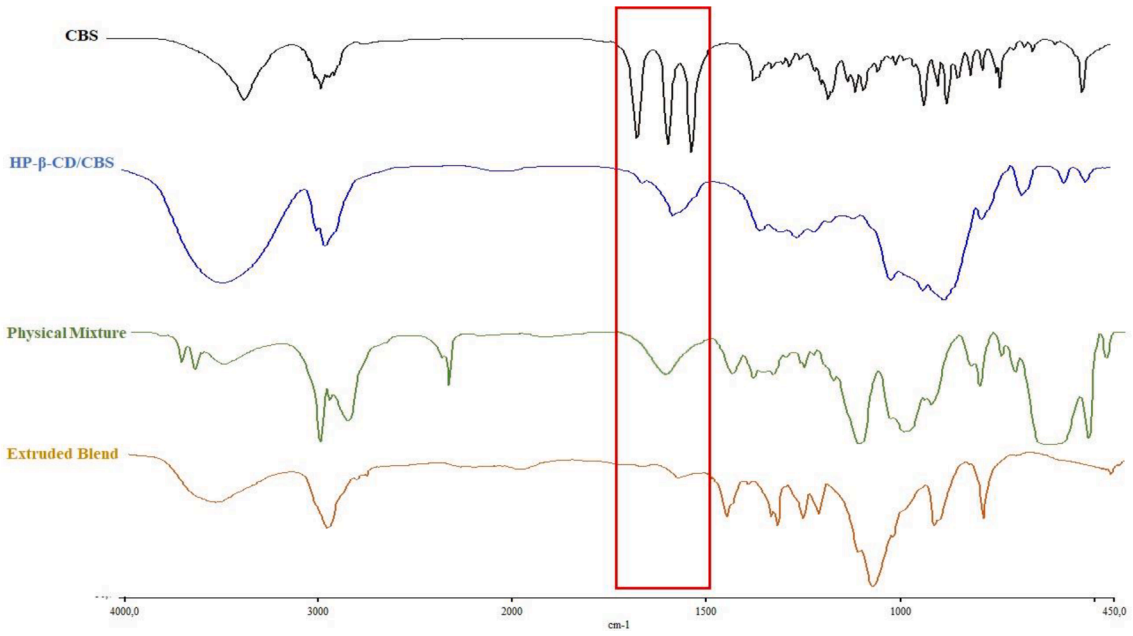

Fig. 7. FT-IR spectra of the printed mucoadhesive films were compared with the spectra of the pure CBS, physical mixture, and HP-β-CD/CBS complex.

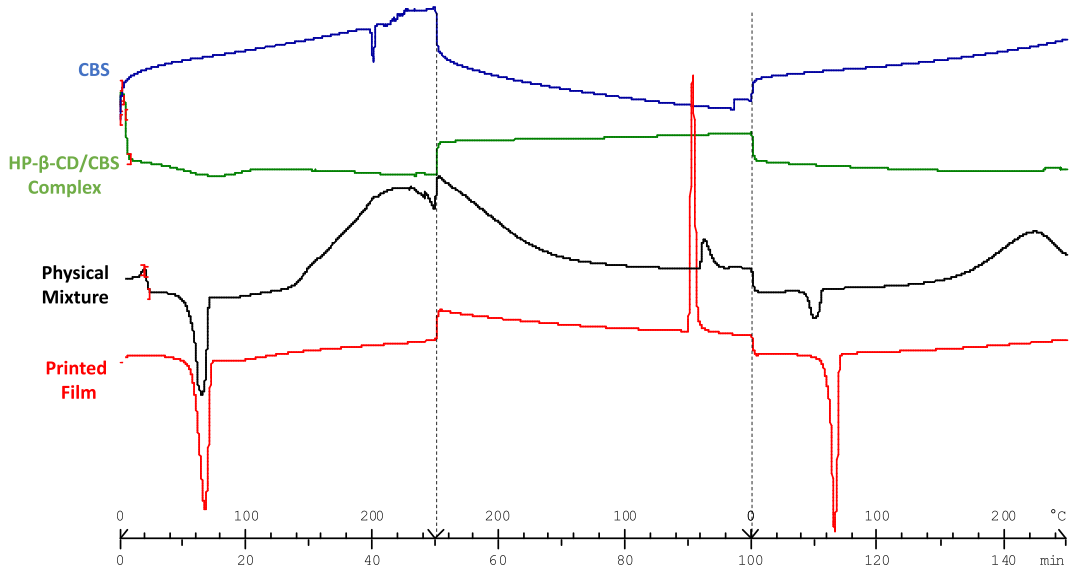

Fig. 8. Thermograms of printed mucoadhesive films were compared with the thermograms of CBS, HP-β-CD/CBS complex, physical mixture, and printed film.

of detachment energy (i.e., AUC), although the significance of these results was weak ($p > 0.50$). On the contrary, other parameters, such as film thickness, seem not impact on the mucoadhesive properties. Comparing the Form. 1 and Form. 2, similar DF values were obtained ($p = 0.98$), suggesting that the number of deposed layers seems not to influence the mucoadhesive properties of the film (Table 4).

Finally, since the films' surfaces showed a different morphology due to the printing process, namely the surface in contact with the printing support resulted in flatter than the other one. In this light, mucoadhesive tests on Form. 3 was also performed to determine the impact of surface morphology irregularities on the mucoadhesive properties. As reported in Table 4, a significant drop of both detachment force ($p = 0.02$) was observable due to a non-optimal contact between the mucin compact and the film due to the rough irregularities present on film surface.

3.8. Tensile properties

Table 5 reported results of tensile test on mucoadhesive films of Form. 1. Forms. 2 and 3 resulted too tough to be analyzed by the texture analyzer. Indeed, for both formulations, the maximum load limit of dynamometer transducer (>40 N) was reached after few seconds from the experiment start. Such positive effect of film thickness on toughness might be connected to the higher of interconnections among film layers deposited during printing process. On the contrary, Form. 1 film showed tensile properties measurable in instrumental range. As well, such films resulted in a higher toughness (TS) and a lower elasticity (Y) in comparison to published data obtained on films prepared using different casting and printing technologies (Khalid et al., 2021; Musazzi et al., 2018a, 2018b).

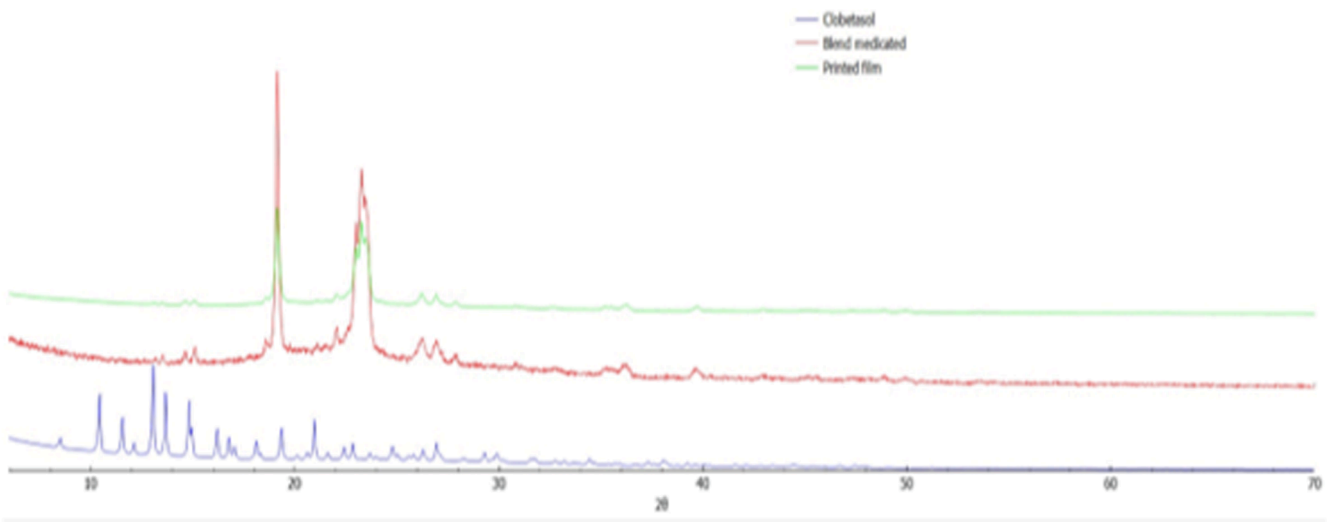

Fig. 9. Diffractograms of the printed mucoadhesive films, each compared with the diffractograms of CBS and the respective medicated blend.

Table 4
Results of mucoadhesive tests performed on mucoadhesive films, expressed as mean ± St.Dev. (n = 3).

Form.	Contact surface	DF_{max} (N/mm^2)	AUC (mJ)
1	Flat	60.67 ± 1.65	0.879 ± 0.231
2	Flat	59.79 ± 4.27	0.761 ± 0.388
3	Flat	74.14 ± 2.92	1.027 ± 0.687
3	Rough	63.32 ± 1.69	0.520 ± 0.055

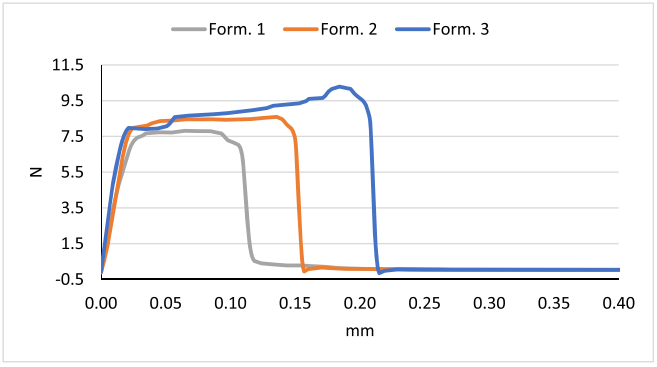

Fig. 10. Representative detachment profiles of three batches.

Table 5
Results of tensile tests performed on mucoadhesive films, expressed as mean ± St.Dev. (n = 8).

Parameter	Form. 1
TS (MPa)	3.93 ± 1.32
E%	4.82 ± 1.98
Y (MPa)	291.85 ± 71.56
TBE (Mpa)	0.093 ± 0.038

3.9. In vitro permeation and retention studies

As reported in Table 6, for both tested formulations the drug permeated amounts resulted negligible at the end of the experiment. On the contrary, about 0.5–0.6 μg/cm^2 of CBS (corresponding to 0.3–0.5 μg/mg of epithelium) was retained in the esophageal mucosa after 7 h. Such finding was in line with published results by using different type of

Table 6
Penetration data (e.g., $Q_{7h,perm}$, $Q_{7h,ret}$) of CBS through esophageal epithelium (mean ± St.Dev., n = 3).

Formulation	$Q_{7h,perm}$ (μg/cm^2)	$Q_{7h,ret}$ (μg/mg)
Blend 2	n.d.	0.518 ± 0.100
Blend 3	n.d.	0.376 ± 0.091

n.d.: not determinable since drug concentration lower than LOD.

mucoadhesive films (Said et al., 2021). However, it's noteworthy noting that, based on obtained results, CS has a role in penetration of CBS into the epithelium. In particular, the higher the CS concentration, the lower the $Q_{7h,ret}$ (p-value = 0.003, Student's T Test).

3.10. Ex vivo mucoadhesive and dissolution studies

Dissolution studies were performed on a film sample placed on the animal mucosae (porcine esophagus), following the wash-off method. The dissolution of the samples was followed by visual analysis at different time intervals (1, 5, 10, 15, 20, 25 and 30 min). The analyzed samples produced by Blend 2 and Blend 3 showed gradual disintegration until complete dissolution 20 min and 30 min after the start of the test, respectively. At the same time, the mucoadhesion of the sample was assessed by the amount of drug still present on the mucosae after washing with simulated salivary fluid. From the results shown in Fig. 11, it was noted that in both cases the medicated mucoadhesive films showed a gradual release of the drug over time and a significant increase in the amount of CBS present in the mucosae compared with the control

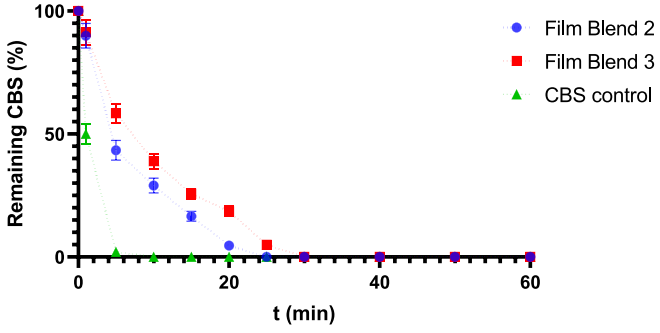

Fig. 11. Mucoadhesion profile of CBS loaded mucoadhesive films on oesophagus mucosae.

sample consisting of the drug alone. This behavior is due to the interaction of CS and PEO with the mucosal surface, which increases the drug's resistance to scavenging, resulting in a longer residence time of the drug at the site of action. The sample derived from Blend 3 showed greater resistance to scavenging and thus better mucoadhesive property resulting from the higher presence of CS, hence the higher number of bonds with the mucosal surface.

3.11. Stability studies

The amorphous condition of the drug, initially acquired by the printing process, was checked after 3 months under controlled storage parameters (25 °C, 60% RH), showing no changes in the solid state of the compounds and the drug content, thus indicating the 3-month stability of the obtained films.

4. Conclusions

The main objective of this work was to develop a novel mucoadhesive film obtained by 3D printing DPE technique capable of giving sustained release of CBS within paediatric OLP therapy. In the obtained formulations, the chemical-physical characteristics of the drug were effectively improved due to the partial amorphization of the drug during the printing stage and owing to the formation of a cyclodextrins multicomponent complex. From the tests performed, the obtained mucoadhesive films exhibited high mucoadhesive properties, improving with increasing CS percentage inside them, an elastic and tenacious structure, and marked retention of the drug inside the epithelium, thus avoiding systemic absorption of the drug. Therefore, mucoadhesive films could represent a suitable candidate in the paediatric therapy of OLP.

CRediT authorship contribution statement

Giuseppe Francesco Racaniello: Writing – original draft, Conceptualization, Data curation. **Monica Pistone:** Data curation, Methodology. **Chiara Meazzini:** Data curation, Methodology. **Angela Lopedota:** Validation, Writing – review & editing. **Ilaria Arduino:** Investigation, Data curation. **Rosanna Rizzi:** Formal Analysis, Data curation. **Antonio Lopalco:** Validation, Writing – review & editing. **Umberto Musazzi:** Writing – original draft, Conceptualization. **Francesco Cilurzo:** Writing – review & editing, Validation, Supervision. **Nunzio Denora:** Writing – review & editing, Validation, Supervision.

Declaration of Competing Interest

The authors declare that they have no known competing financial interests or personal relationships that could have appeared to influence the work reported in this paper.

Data availability

Data will be made available on request.

Acknowledgments

We would like to thank Siciliani S.p.A. (Palo del Colle, BA, Italy) to provide us the porcine esophagus. The authors would also like to thank the P.O.N "Ricerca e Innovazione" 2014-2020 - Fondi D.M. 1062/2021.

References

Azad, M.A., Olawuni, D., Kimbell, G., Badruddoza, A.Z.M., Hossain, M.S., Sultana, T., 2020. Polymers for extrusion-based 3D printing of pharmaceuticals: A holistic materials–process perspective. Pharmaceutics. https://doi.org/10.3390/pharmaceutics12020124.

Bernkop-Schnürch, A., 2005. Thiomers: a new generation of mucoadhesive polymers. Adv. Drug Deliv. Rev. 57, 1569–1582. https://doi.org/10.1016/j.addr.2005.07.002.

Boniatti, J., Januskaite, P., da Fonseca, L.B., Viçosa, A.L., Amendoeira, F.C., Tuleu, C., Basit, A.W., Goyanes, A., Ré, M.-I., 2021. Direct Powder Extrusion 3D Printing of Praziquantel to Overcome Neglected Disease Formulation Challenges in Paediatric Populations. Pharmaceutics 13, 1114. https://doi.org/10.3390/pharmaceutics13081114.

Boorghani, M., Gholizadeh, N., Zenouz, A.T., Vatankhah, M., Mehdipour, M., 2010. Oral lichen planus: clinical features, etiology, treatment and management; a review of literature. J. Dent. Res. Dent. Clin. Dent. Prospects 4, 3.

Byyny, R.L., 1976. Withdrawal from glucocorticoid therapy. N. Engl. J. Med. 295, 30–32. https://doi.org/10.1056/NEJM197607012950107.

Canto, A.M. do, Müller, H., Freitas, R.R. de, Santos, P.S. da S., 2010. Oral lichen planus (OLP): clinical and complementary diagnosis. An Bras Dermatol. 85, 669–675.

Carbone, M., Arduino, P.G., Carrozzo, M., Caiazzo, G., Broccoletti, R., Conrotto, D., Bezzo, C., Gandolfo, S., 2009. Topical clobetasol in the treatment of atrophic-erosive oral lichen planus: a randomized controlled trial to compare two preparations with different concentrations. J. Oral Pathol. Med. 38, 227–233. https://doi.org/10.1111/j.1600-0714.2008.00688.x.

Carruthers, J.A., August, P.J., Staughton, R.C., 1975. Observations on the systemic effect of topical clobetasol propionate (Dermovate). Br. Med. J. 4, 203–204. https://doi.org/10.1136/bmj.4.5990.203.

Casiraghi, A., Gennari, C.G., Musazzi, U.M., Ortenzi, M.A., Bordignon, S., Minghetti, P., 2020. Mucoadhesive Budesonide Formulation for the Treatment of Eosinophilic Esophagitis. Pharmaceutics 12. https://doi.org/10.3390/pharmaceutics12030211.

Cheung, R.C.F., Ng, T.B., Wong, J.H., Chan, W.Y., 2015. Chitosan: An Update on Potential Biomedical and Pharmaceutical Applications. Mar. Drugs 13, 5156–5186. https://doi.org/10.3390/md13085156.

Chung, S., Srinivasan, P., Zhang, P., Bandari, S., Repka, M.A., 2022. Development of ibuprofen tablet with polyethylene oxide using fused deposition modeling 3D-printing coupled with hot-melt extrusion. J. Drug Deliv. Sci. Technol. 76, 103716 https://doi.org/10.1016/j.jddst.2022.103716.

Cilurzo, F., Minghetti, P., Selmin, F., Casiraghi, A., Montanari, L., 2003. Polymethacrylate salts as new low-swellable mucoadhesive materials. J. Control. Release 88, 43–53. https://doi.org/10.1016/S0168-3659(02)00459-5.

Cilurzo, F., Gennari, C.G.M., Selmin, F., Epstein, J.B., Gaeta, G.M., Colella, G., Minghetti, P., 2010. A new mucoadhesive dosage form for the management of oral lichen planus: Formulation study and clinical study. Eur. J. Pharm. Biopharm. 76, 437–442. https://doi.org/10.1016/j.ejpb.2010.07.014.

Cutrignelli, A., Lopedota, A., Denora, N., Iacobazzi, R.M., Fanizza, E., Laquintana, V., Perrone, M., Maggi, V., Franco, M., 2014. A New Complex of Curcumin with Sulfobutylether-β-Cyclodextrin: Characterization Studies and In Vitro Evaluation of Cytotoxic and Antioxidant Activity on HepG-2 Cells. J. Pharm. Sci. 103, 3932–3940. https://doi.org/10.1002/jps.24200.

Cuzzolin, L., Zaccaron, A., Fanos, V., 2003. Unlicensed and off-label uses of drugs in paediatrics: a review of the literature. Fundam. Clin. Pharmacol. 17, 125–131. https://doi.org/10.1046/j.1472-8206.2003.00123.x.

d'Angelo, I., Fraix, A., Ungaro, F., Quaglia, F., Miro, A., 2017. Poly(ethylene oxide)/hydroxypropyl-β-cyclodextrin films for oromucosal delivery of hydrophilic drugs. Int. J. Pharm. 531, 606–613. https://doi.org/10.1016/j.ijpharm.2017.06.029.

Dores, F., Kuźmińska, M., Soares, C., Bohus, M., Shervington, A.L., Habashy, R., Pereira, B.C., Peak, M., Isreb, A., Alhnan, M.A., 2020. Temperature and solvent facilitated extrusion based 3D printing for pharmaceuticals. Eur. J. Pharm. Sci. 152, 105430 https://doi.org/10.1016/j.ejps.2020.105430.

Eversole, L.R., 1997. Immunopathogenesis of oral lichen planus and recurrent aphthous stomatitis. In: Seminars in Cutaneous Medicine and Surgery. pp. 284–294.

Fanous, M., Gold, S., Muller, S., Hirsch, S., Ogorka, J., Imanidis, G., 2020. Simplification of fused deposition modeling 3D-printing paradigm: Feasibility of 1-step direct powder printing for immediate release dosage form production. Int. J. Pharm. 578, 119124 https://doi.org/10.1016/j.ijpharm.2020.119124.

Ferguson, M.M., 1977. Treatment of erosive lichen planus of the oral mucosa with depot steroids. Lancet. https://doi.org/10.1016/s0140-6736(77)90288-4.

Garipova, V., Gennari, C., Selmin, F., Cilurzo, F., Moustafine, R., 2018. Mucoadhesive Interpolyelectrolyte Complexes for the Buccal Delivery of Clobetasol. Polymers (Basel) 10, 85. https://doi.org/10.3390/polym10010085.

Goyanes, A., Allahham, N., Trenfield, S.J., Stoyanov, E., Gaisford, S., Basit, A.W., 2019. Direct powder extrusion 3D printing: Fabrication of drug products using a novel single-step process. Int. J. Pharm. 567, 118471 https://doi.org/10.1016/j.ijpharm.2019.118471.

Jiang, W.-Z., Cai, Y., Li, H.-Y., 2017. Chitosan-based spray-dried mucoadhesive microspheres for sustained oromucosal drug delivery. Powder Technol. 312, 124–132. https://doi.org/10.1016/j.powtec.2017.02.021.

Kamberi, M., Fu, K., Lu, J., Chemaly, G.M., Feder, D., 2008. A sensitive high-throughput HPLC assay for simultaneous determination of everolimus and clobetasol propionate. J. Chromatogr. Sci. 46, 23–29. https://doi.org/10.1093/chromsci/46.1.23.

Khalid, G.M., Musazzi, U.M., Selmin, F., Franzè, S., Minghetti, P., Cilurzo, F., 2021. Extemporaneous printing of diclofenac orodispersible films for pediatrics. Drug Dev. Ind. Pharm. 1–9. https://doi.org/10.1080/03639045.2021.1908335.

Laeijendecker, R., Van Joost, T., Tank, B., Oranje, A.P., Neumann, H.A.M., 2005. Oral Lichen Planus in Childhood. Pediatr. Dermatol. 22, 299–304. https://doi.org/10.1111/j.1525-1470.2005.22403.x.

Lafeber, I., Ruijgrok, E.J., Guchelaar, H.-J., Schimmel, K.J.M., 2022. 3D Printing of Pediatric Medication: The End of Bad Tasting Oral Liquids?—A Scoping Review. Pharmaceutics 14, 416. https://doi.org/10.3390/pharmaceutics14020416.

Liu, S., Qin, S., He, M., Zhou, D., Qin, Q., Wang, H., 2020. Current applications of poly (lactic acid) composites in tissue engineering and drug delivery. Compos. B Eng. 199, 108238 https://doi.org/10.1016/j.compositesb.2020.108238.

Lodagekar, A., Borkar, R.M., Thatikonda, S., Chavan, R.B., Naidu, V.G.M., Shastri, N.R., Srinivas, R., Chella, N., 2019. Formulation and evaluation of cyclodextrin complexes for improved anticancer activity of repurposed drug: Niclosamide. Carbohydr. Polym. 212, 252–259. https://doi.org/10.1016/j.carbpol.2019.02.041.

Loftsson, T., Hreinsdóttir, D., Másson, M., 2005. Evaluation of cyclodextrin solubilization of drugs. Int. J. Pharm. 302, 18–28. https://doi.org/10.1016/j.ijpharm.2005.05.042.

Mašková, E., Kubová, K., Raimi-Abraham, B.T., Vllasaliu, D., Vohlídalová, E., Turánek, J., Mašek, J., 2020. Hypromellose – A traditional pharmaceutical excipient with modern applications in oral and oromucosal drug delivery. J. Control. Release 324, 695–727. https://doi.org/10.1016/j.jconrel.2020.05.045.

Medarević, D., Kachrimanis, K., Djurić, Z., Ibrić, S., 2015. Influence of hydrophilic polymers on the complexation of carbamazepine with hydroxypropyl-β-cyclodextrin. Eur. J. Pharm. Sci. 78, 273–285. https://doi.org/10.1016/j.ejps.2015.08.001.

Morales, J.O., McConville, J.T., 2011. Manufacture and characterization of mucoadhesive buccal films. Eur. J. Pharm. Biopharm. 77, 187–199. https://doi.org/10.1016/J.EJPB.2010.11.023.

Morath, B., Sauer, S., Zaradzki, M., Wagner, A.H., 2022. Orodispersible films – Recent developments and new applications in drug delivery and therapy. Biochem. Pharmacol. 200, 115036 https://doi.org/10.1016/j.bcp.2022.115036.

Musazzi, U.M., Selmin, F., Franzé, S., Gennari, C.G.M., Rocco, P., Minghetti, P., Cilurzo, F., 2018a. Poly(methyl methacrylate) salt as film forming material to design orodispersible films. Eur. J. Pharm. Sci. 115, 37–42. https://doi.org/10.1016/j.ejps.2018.01.019.

Musazzi, U.M., Selmin, F., Ortenzi, M.A., Mohammed, G.K., Franzé, S., Minghetti, P., Cilurzo, F., 2018b. Personalized orodispersible films by hot melt ram extrusion 3D printing. Int. J. Pharm. 551, 52–59. https://doi.org/10.1016/J.IJPHARM.2018.09.013.

Nair, A.B., Kumar, S., Dalal, P., Nagpal, C., Dalal, S., Rao, R., Sreeharsha, N., Jacob, S., 2022. Novel Dermal Delivery Cargos of Clobetasol Propionate: An Update. Pharmaceutics. https://doi.org/10.3390/pharmaceutics14020383.

Ong, J.J., Awad, A., Martorana, A., Gaisford, S., Stoyanov, E., Basit, A.W., Goyanes, A., 2020. 3D printed opioid medicines with alcohol-resistant and abuse-deterrent properties. Int. J. Pharm. 579, 119169 https://doi.org/10.1016/j.ijpharm.2020.119169.

Oussedik, E., Saleem, M.D., Feldman, S.R., 2017. A Randomized, Double-Blind, Placebo-Controlled Study of the Vasoconstrictor Potency of Topical 0.25% Desoximetasone Spray: A High to Super High Range of Potency (Class I to Class II) Corticosteroid Formulation. J. Drugs Dermatol. 16, 972–975.

Palezi, S.C., Fernandes, S.S., Martins, V.G., 2022. Oral disintegration films: applications and production methods. J. Food Sci. Technol. https://doi.org/10.1007/s13197-022-05589-9.

Pandey, M., Choudhury, H., Fern, J.L.C., Kee, A.T.K., Kou, J., Jing, J.L.J., Her, H.C., Yong, H.S., Ming, H.C., Bhattamisra, S.K., Gorain, B., 2020. 3D printing for oral drug delivery: a new tool to customize drug delivery. Drug Deliv. Transl. Res. 10, 986–1001. https://doi.org/10.1007/s13346-020-00737-0.

Pistone, M., Racaniello, G.F., Arduino, I., Laquintana, V., Lopalco, A., Cutrignelli, A., Rizzi, R., Franco, M., Lopedota, A., Denora, N., 2022. Direct cyclodextrin-based powder extrusion 3D printing for one-step production of the BCS class II model drug niclosamide. Drug Deliv. Transl. Res. 12, 1895–1910. https://doi.org/10.1007/s13346-022-01124-7.

Pistone, M., Racaniello, G.F., Rizzi, R., Iacobazzi, R.M., Arduino, I., Lopalco, A., Lopedota, A.A., Denora, N., 2023. Direct cyclodextrin based powder extrusion 3D printing of budesonide loaded mini-tablets for the treatment of eosinophilic colitis in paediatric patients. Int. J. Pharm. 632, 122592 https://doi.org/10.1016/j.ijpharm.2023.122592.

Plemons, J.M., Rees, T.D., Zachariah, N.Y., 1990. Absorption of a topical steroid and evaluation of adrenal suppression in patients with erosive lichen planus. Oral Surg. Oral Med. Oral Pathol. 69, 688–693. https://doi.org/10.1016/0030-4220(90)90349-w.

Polamaplly, P., Cheng, Y., Shi, X., Manikandan, K., Kremer, G.E., Qin, H., 2019. 3D Printing and Characterization of Hydroxypropyl Methylcellulose and Methylcellulose for Biodegradable Support Structures. Procedia Manuf 34, 552–559. https://doi.org/10.1016/j.promfg.2019.06.219.

Preis, M., Breitkreutz, J., Sandler, N., 2015. Perspective: Concepts of printing technologies for oral film formulations. Int. J. Pharm. 494, 578–584. https://doi.org/10.1016/j.ijpharm.2015.02.032.

Racaniello, G.F., Laquintana, V., Summonte, S., Lopedota, A., Cutrignelli, A., Lopalco, A., Franco, M., Bernkop-Schnürch, A., Denora, N., 2021. Spray-dried mucoadhesive microparticles based on S-protected thiolated hydroxypropyl-β-cyclodextrin for budesonide nasal delivery. Int. J. Pharm. 603, 120728 https://doi.org/10.1016/j.ijpharm.2021.120728.

Rincón-López, J., Almanza-Arjona, Y.C., Riascos, A.P., Rojas-Aguirre, Y., 2021. Technological evolution of cyclodextrins in the pharmaceutical field. J. Drug Deliv. Sci. Technol. 61, 102156 https://doi.org/10.1016/j.jddst.2020.102156.

Russo, E., Selmin, F., Baldassari, S., Gennari, C.G.M., Caviglioli, G., Cilurzo, F., Minghetti, P., Parodi, B., 2016. A focus on mucoadhesive polymers and their application in buccal dosage forms. J. Drug Deliv. Sci. Technol. 32, 113–125. https://doi.org/10.1016/j.jddst.2015.06.016.

Said, Z., Murdoch, C., Hansen, J., Siim Madsen, L., Colley, H.E., 2021. Corticosteroid delivery using oral mucosa equivalents for the treatment of inflammatory mucosal diseases. Eur. J. Oral Sci. 129, e12761.

Salamat-Miller, N., Chittchang, M., Johnston, T.P., 2005. The use of mucoadhesive polymers in buccal drug delivery. Adv. Drug Deliv. Rev. 57, 1666–1691. https://doi.org/10.1016/j.addr.2005.07.003.

Sarfaraz Alam, M., Ali, M.S., Zakir, F., Alam, N., Intakhab Alam, M., Ahmad, F., Siddiqui, M.R., Ali, M.D., Ansari, M.S., Ahmad, S., Ali, M., 2016. Enhancement of Anti-Dermatitis Potential of Clobetasol Propionate by DHA [Docosahexaenoic Acid] Rich Algal Oil Nanoemulsion Gel. Iran J. Pharm. Res. 15, 35–52.

Scarpa, M., Stegemann, S., Hsiao, W.-K., Pichler, H., Gaisford, S., Bresciani, M., Paudel, A., Orlu, M., 2017. Orodispersible films: Towards drug delivery in special populations. Int. J. Pharm. 523, 327–335. https://doi.org/10.1016/j.ijpharm.2017.03.018.

Spath, S., Seitz, H., 2014. Influence of grain size and grain-size distribution on workability of granules with 3D printing. Int. J. Adv. Manuf. Technol. 70, 135–144. https://doi.org/10.1007/s00170-013-5210-8.

Tejada, G., Barrera, M.G., Piccirilli, G.N., Sortino, M., Frattini, A., Salomón, C.J., Lamas, M.C., Leonardi, D., 2017. Development and Evaluation of Buccal Films Based on Chitosan for the Potential Treatment of Oral Candidiasis. AAPS PharmSciTech 18, 936–946. https://doi.org/10.1208/s12249-017-0720-6.

Thiry, J., Krier, F., Ratwatte, S., Thomassin, J.-M., Jerome, C., Evrard, B., 2017. Hot-melt extrusion as a continuous manufacturing process to form ternary cyclodextrin inclusion complexes. Eur. J. Pharm. Sci. 96, 590–597. https://doi.org/10.1016/j.ejps.2016.09.032.

Wei, C., Solanki, N.G., Vasoya, J.M., Shah, A.V., Serajuddin, A.T.M., 2020. Development of 3D Printed Tablets by Fused Deposition Modeling Using Polyvinyl Alcohol as Polymeric Matrix for Rapid Drug Release. J. Pharm. Sci. 109, 1558–1572. https://doi.org/10.1016/j.xphs.2020.01.015.

Zema, L., Melocchi, A., Maroni, A., Gazzaniga, A., 2017. Three-Dimensional Printing of Medicinal Products and the Challenge of Personalized Therapy. J. Pharm. Sci. 106, 1697–1705. https://doi.org/10.1016/j.xphs.2017.03.021.